Monte Carlo simulations of stress relaxation of entanglement-free Fraenkel chains. I. Linear polymer viscoelasticity

Y.-H. Lin and A. K. Das

Citation: The Journal of Chemical Physics **126**, 074902 (2007); doi: 10.1063/1.2431648
View online: http://dx.doi.org/10.1063/1.2431648
View Table of Contents: http://scitation.aip.org/content/aip/journal/jcp/126/7?ver=pdfcov
Published by the AIP Publishing

Monte Carlo simulations of stress relaxation of entanglement-free Fraenkel chains. I. Linear polymer viscoelasticity

Y.-H. Lin[a] and A. K. Das
Department of Applied Chemistry, National Chiao Tung University, Hsinchu 30050, Taiwan

(Received 2 October 2006; accepted 12 December 2006; published online 15 February 2007)

Shear stress relaxation modulus $G_S(t)$ curves of entanglement-free Fraenkel chains have been calculated using Monte Carlo simulations based on the Langevin equation, carrying out both in the equilibrium state and following the application of a step shear deformation. While the fluctuation-dissipation theorem is perfectly demonstrated in the Rouse-chain model, a quasiversion of the fluctuation-dissipation theorem is observed in the Fraenkel-chain model. In both types of simulations on the Fraenkel-chain model, two distinct modes of dynamics emerge in $G_S(t)$, giving a line shape similar to that typically observed experimentally. Analyses show that the fast mode arises from the segment-tension fluctuations or reflects the relaxation of the segment tension created by segments being stretched by the applied step strain—an energetic-interactions-driven process—while the slow mode arises from the fluctuations in segmental orientation or represents the randomization of the segmental-orientation anisotropy induced by the step deformation—an entropy-driven process. Furthermore, it is demonstrated that the slow mode is well described by the Rouse theory in all aspects: the magnitude of modulus, the line shape of the relaxation curve, and the number-of-beads (N) dependence of the relaxation times. In other words, one Fraenkel segment substituting for one Rouse segment, it has been shown that the entropic-force constant on each segment is not a required element to give rise to the Rouse modes of motion, which describe the relaxation modulus of an entanglement-free polymer over the long-time region very well. This conclusion provides an explanation resolving a long-standing fundamental paradox in the success of Rouse-segment-based molecular theories for polymer viscoelasticity—namely, the paradox between the Rouse segment size being of the same order of magnitude as that of the Kuhn segment (each Fraenkel segment with a large force constant H_F can be regarded as basically equivalent to a Kuhn segment) and the meaning of the Rouse segment as defined in the Rouse-chain model. The general agreement observed in the comparison of the simulation and experimental results indicates that the Fraenkel-chain model, while being still relatively simple, has captured the key element in energetic interactions—the rigidity on the segment—in a polymer system. © *2007 American Institute of Physics*. [DOI: 10.1063/1.2431648]

I. INTRODUCTION

It has been shown that many aspects of the linear viscoelasticity of an entanglement-free polymer melt is well described by the Rouse theory.[1–5] In a viscoelastic spectrum, the agreement between theory and experiment is limited to the region below the modulus level corresponding to the molecular weight of a single Rouse segment that can be assigned to the polymer system—for instance, below $\sim \rho RT/m = 3.8 \times 10^7$ dyn/cm^2, corresponding to the Rouse-segmental molecular weight $m \approx 850$ in the case of polystyrene.[6–16] In other words, the agreement occurs only in the frequency region slower than the motion associated with a single Rouse segment or equivalently the relaxation rate of the highest Rouse mode. Because of the entropic-force constant on the Rouse segment, this region may be referred to as the entropic region and the relaxation processes in it as entropy-driven dynamics. The entire viscoelastic spectrum in the entropic region follows the same temperature dependence, indicating that thermorheological simplicity is followed in the region. This is expected from the Rouse theory; namely, the frictional factor associated with the Rouse segment carries the temperature dependence of the viscoelastic behavior. In the frequency region faster than the motion of a single Rouse segment, the modulus of the relaxation process is much higher—ranging from $\sim 4 \times 10^7$ to $\sim 10^{10}$ dyn/cm^2 for polystyrene. The high modulus is due to the strong energetic interactions among segments, both intrachain and interchain; the segmental motions in this region may be properly referred to as energetic-interactions-driven dynamics, which has also been referred to in the literature as the glassy relaxation or the structural relaxation or the α relaxation. It has been widely observed that as the temperature approaches the glass transition temperature T_g from above, the energetic-interactions-driven dynamics has a temperature dependence stronger than that of the entropy driven.[17–24] Thus, when the whole range of the viscoelastic response (relaxation modulus, viscoelastic spectrum, or creep compliance) is taken into consideration, the thermorheological simplicity does not hold. Recently, the basic mechanism for the thermorheologi-

[a]Electronic mail: yhlin@mail.nctu.edu.tw

cal complexity in polystyrene has been analyzed, showing that the effect as related to T_g behaves in a universal way within the polystyrene system, entangled or not.[15,25] While it has been extensively shown that the Rouse-segment-based molecular theories, the Rouse theory[1–5] for the entanglement-free system and the extended reptation theory[3,15,26–28] (ERT) for the entangled system, describe the viscoelastic responses in the entropic region successfully in a quantitative way, the structural-relaxation process can only be analyzed phenomenologically, often in terms of a stretched exponential form. In other words, we have a quite limited understanding of the structural-relaxation process at the molecular level. In this study, using the Monte Carlo simulation based on the Langevin equation,[3,14] we compute the relaxation modulus curves of the model systems which contain a proper kind of interaction potential—the Fraenkel chains,[29] shedding light on the coexistence of and the interrelation between the energetic-interactions-driven and entropy-driven dynamic processes.

II. MONTE CARLO SIMULATION OF THE LANGEVIN EQUATION

In the Monte Carlo simulation, the continuous change in time, dt, in the Langevin equation is replaced by a small time step, Δt. For a chain with the positions of the beads at time step i denoted by $\{\mathbf{R}_n(i)\}$, the simulation form of the Langevin equation is expressed by

$$\mathbf{R}_n(i+1) = \mathbf{R}_n(i) + \frac{d^2}{2}\left(\frac{\mathbf{F}_n(i)}{kT}\right) + \mathbf{d}_n(i), \tag{1}$$

where $\mathbf{F}_n(i)$ is the force on the nth bead at the ith time step arising from the interaction potential; the random step vector $\mathbf{d}_n(i)$ is characterized by the following first and second moments:

$$\langle \mathbf{d}_n(i) \rangle = 0 \tag{2}$$

and

$$\langle \mathbf{d}_n(i)\mathbf{d}_m(j) \rangle = d^2\mathbf{I}\delta_{nm}\delta_{ij}, \tag{3}$$

with $\mathbf{I}$ being a unit tensor.

Then the relaxation modulus can be calculated from the Monte Carlo simulation after a step shear deformation

$$\mathbf{E} = \begin{pmatrix} 1 & \lambda & 0 \\ 0 & 1 & 0 \\ 0 & 0 & 1 \end{pmatrix} \tag{4}$$

is applied to the polymer chain in an equilibrium state at $t=0$. Following the application of the step deformation $\mathbf{E}$, the evolution of $\{\mathbf{R}_n(i)\}$ is calculated according to Eq. (1), and the stress relaxation of a chain with N beads, normalized to per segment, is given by

$$S_{xy}(\lambda, i) = \frac{1}{(N-1)}\sum_{n=1}^{N} \langle F_{nx}(i)Y_n(i) \rangle. \tag{5}$$

For the simulation, a large number of identical relaxation processes following a step deformation are repeated and accumulated for averaging, as denoted by the angular brackets in Eq. (5). Before a new cycle is repeated, the system must run for a sufficiently large number of time steps to reach an equilibrium state. To prevent some residual memory from accumulating, the step deformation may be applied in a cyclic manner, as done in this study; if the $\mathbf{E}$ given by Eq. (4) is referred to as a deformation in the x direction and denoted by x, the deformation cycle $x \to -x \to y \to -y \to z \to -z$ is repeated and following each step deformation, the physically equivalent stress component is collected for averaging. Although the cyclic scheme is used for averaging throughout the simulation study as reported in this paper and the companion paper,[30] to conveniently discuss the anisotropy introduced by the deformation, the obtained results will be discussed with respect to Eq. (4) as the chosen direction of deformation—in other words, the shear stress is denoted by the xy component. Denoting the thus averaged shear stress relaxation as $S_{xy}(\lambda, i)$, the relaxation modulus per segment is given by

$$G_S(i) = -\frac{S_{xy}(\lambda, i)}{\lambda}. \tag{6}$$

In this study, we are mainly interested in the linear relaxation modulus. In accordance with the fluctuation-dissipation theorem, the relaxation modulus equivalent to that given by Eq. (6) in the linear region of λ can be calculated from[31–33]

$$G_S(i) = \frac{1}{6(N-1)kT}\sum_{\alpha\neq\beta} \langle J_{\alpha\beta}(0)J_{\alpha\beta}(i) \rangle$$

$$= \frac{1}{6I(N-1)kT}\sum_{i_0=1}^{I}\sum_{\alpha\neq\beta} J_{\alpha\beta}(i_0)J_{\alpha\beta}(i_0+i), \tag{7}$$

with α, β denoting x, y, z, where

$$J_{xy}(i) = \sum_{n=1}^{N} F_{nx}(i)Y_n(i), \tag{8}$$

and I represents a large number of iteration (typically $\sim 10^4$). Although in the simulation we use all the six combinations of $J_{\alpha\beta}(t)$ (with $\alpha \neq \beta$) for averaging in calculating the time-correlation function, in our discussion below, we shall use the xy component as the representative of the shear stress. The simulation result as obtained through Eq. (6) is referred to as the step-strain-simulation $G_S(t)$, as opposed to the equilibrium-simulation $G_S(t)$ obtained through Eq. (7).

For a Rouse chain, the force on an internal bead is given by[2,3]

$$\mathbf{F}_n(i) = -\frac{3kT}{\langle b^2 \rangle}(2\mathbf{R}_n(i) - \mathbf{R}_{n+1}(i) - \mathbf{R}_{n-1}(i)). \tag{9}$$

An equivalent equation can be written for the end beads: $n=1$ or N. Throughout our calculations we have set $\langle b^2 \rangle = 1$.

The relaxation modulus contributed by a single Rouse chain—averaged in a mean field—with N beads or molecular weight M is given by[2,3]

$$kT\mu_R(t, M) = kT\sum_{p=1}^{N-1} \exp\left(-\frac{t}{\tau_p}\right), \tag{10}$$

where the relaxation time of the pth normal mode, τ_p, is given by

$$\tau_p = \frac{\zeta\langle b^2\rangle}{24kT\sin^2(p\pi/2N)} = \frac{K\pi^2M^2}{24N^2\sin^2(p\pi/2N)}, \tag{11}$$

with $K=\zeta\langle b^2\rangle/kT\pi^2m^2$ being the frictional factor associated with the Rouse segment.[3] The frictional factor carries the temperature dependence of the relaxation times of a polymer in the entropic region of its relaxation modulus, which is usually described by the Vogel–Fulcher–Tammann equation or the Williams–Landel–Ferry equation.[34–36] In the simulation the time step depends on the step length d chosen; the relaxation time τ_p is expressed in terms of the time step as[14]

$$\frac{\tau_p}{\Delta t} = \frac{\langle b^2\rangle}{12d^2\sin^2(p\pi/2N)}. \tag{12}$$

For a chain whose nearest neighboring beads interact through the Fraenkel potential:

$$U_F = \frac{H_F}{2}\sum_{n=1}^{N-1}\left(\frac{|\mathbf{r}_n-\mathbf{r}_{n+1}|}{b_0}-1\right)^2, \tag{13}$$

the force on an internal bead is given by

$$\mathbf{F}_n(i) = -\frac{H_F}{b_0^2}(2\mathbf{R}_n(i)-\mathbf{R}_{n+1}(i)-\mathbf{R}_{n-1}(i)) + \frac{H_F}{b_0}\left[\frac{\mathbf{R}_n(i)-\mathbf{R}_{n-1}(i)}{|\mathbf{R}_n(i)-\mathbf{R}_{n-1}(i)|}+\frac{\mathbf{R}_n(i)-\mathbf{R}_{n+1}(i)}{|\mathbf{R}_n(i)-\mathbf{R}_{n+1}(i)|}\right]. \tag{14}$$

An equivalent equation can be written for the end beads: $n=1$ or N. Throughout our calculations, we have set $b_0=1$ and $H_F=400kT$.

III. EQUILIBRIUM SIMULATION $G_S(t)$

A. Rouse chains

Equation (12), expressing the relaxation time in terms of time steps, allows one to compare the simulation $G_S(t)$ curve based on a Rouse chain with that calculated from the analytical equation. In Fig. 1, such a comparison is made for two-bead, five-bead, and ten-bead chains; in the comparison, both the simulated and theoretical results are normalized to that corresponding to one single segment with kT set as 1—namely, $G_S(t)=\mu_R(t)/(N-1)$ [see Eq. (10)]. This way of normalization will be adopted throughout this paper (note that kT is shown in equations of this report to indicate the relationship to entropy or average kinetic energy; however, throughout the simulation as well as in the shown results, kT is set to be 1 or equivalently kT is the unit of energy), except for the comparison between simulation and experiment, where the experimental $G(t)$ will be used. The close superposition without any shift along both the modulus and time-step coordinates as shown in Fig. 1 supports the validity of the simulation.

B. Chains consisting of Fraenkel segments

When the entropic force in the Rouse segment is replaced by that derived from the Fraenkel potential, the stiffness of the segment is greatly enhanced. Because the Fraenkel force is a nonlinear function of the bead positions, an analytical solution cannot be obtained from the corresponding Langevin equation. In this case, the Monte Carlo simulation becomes very important and useful for illustrating how enhancing the stiffness of the segment will affect the viscoelastic response.

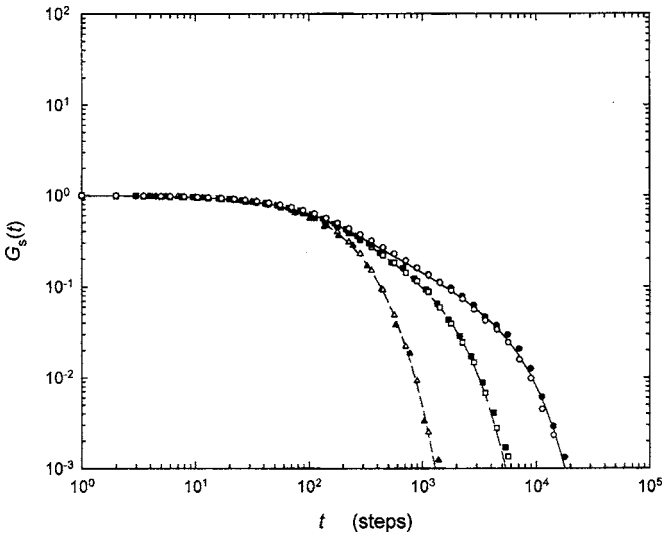

FIG. 1. Comparison of the equilibrium-simulation $G_S(t)$ curves of two-bead, five-bead, and ten-bead Rouse chains (△ for $N=2$, □ for $N=5$, and ○ for $N=10$) with the step-strain-simulation $G_S(t)$ results (▲ for $N=2$, ■ for $N=5$, and ● for $N=10$) and the Rouse theoretical curves (--- for $N=2$, – – – for $N=5$, and — for $N=10$).

The simulations based on chains consisting of Fraenkel segments (referred to as Fraenkel chains below) give rise to two distinct modes in $G_S(t)$ as shown in Fig. 2 for a five-bead chain—the "bead," as in the Rouse-chain model, is actually a volumeless point; with this understanding, we still refer to it as a bead. In Fig. 2, the simulation results obtained with the step length d chosen at 0.01 and 0.03 are compared, with each time step for the latter being treated as nine times—the expected ratio—longer than the one for the former. The close agreement between the two indicates that the step length $d=0.03$ is sufficiently short, causing virtually

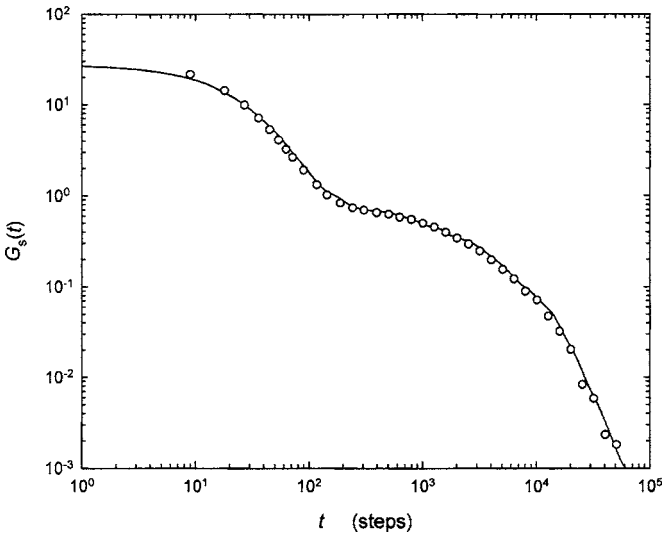

FIG. 2. Comparison of the equilibrium-simulation $G_S(t)$ curves of the five-bead Fraenkel chain using the step lengths $d=0.01$ (—) and $d=0.03$ (○).

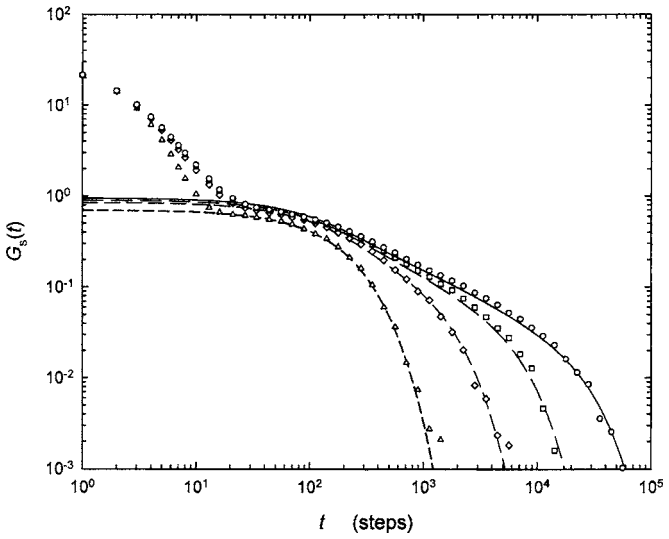

FIG. 3. Comparison of the equilibrium-simulation $G_S(t)$ curves of 2-bead, 5-bead, 10-bead, and 20-bead Fraenkel chains (△ for $N=2$, ◇ for $N=5$, □ for $N=10$, and ○ for $N=20$) with the Rouse theoretical curves (short dash for $N=2$, medium dash for $N=5$, long dash for $N=10$, and solid line for $N=20$). See the text.

no distortion to the obtained $G_S(t)$ curve; at the same time, no additional information particularly significant can be gained from using the much more time-consuming choice, $d=0.01$. Thus, all of our simulations reported in this study and in the companion paper[30] are based on $d=0.03$. In Fig. 3, the $G_S(t)$ curves for 2-bead, 5-bead, 10-bead, and 20-bead Fraenkel chains are compared; their line shapes are similar to what have been typically observed experimentally. We shall show below that the fast mode is an energetic-interactions-driven dynamic process while the slow mode is an entropy-driven one.

In Fig. 3, the $G_S(t)$ results of simulation in the equilibrium state are compared with the Rouse theoretical curves each for a chain with the corresponding number of beads. To obtain the shown close superposition of the Rouse theoretical curves on the simulation results in the long-time region, we only need to apply small shifting factors to the Rouse curves along the modulus coordinate. The multiplication factors representing the shifts are 0.7, 0.85, 0.9, and 0.95 for the dumbbell, 5-bead chain, 10-bead chain, and 20-bead chain, respectively. The trend indicates that the multiplication factor approaches the "perfect" value 1 as the number of beads increases. The shown close agreement of the slow modes with the Rouse $G_S(t)$ curves with only a small shifting factor in the modulus coordinate strongly indicates that the slow mode is well described by the Rouse theory; significantly, the N dependence of the relaxation time as given by Eq. (12) is well followed. Such agreements mean that the slow mode is of entropic nature as the Rouse modes of motion. Considering the fact that the potential function on the Fraenkel segment represents a strong energetic interaction between two beads—much stiffer than the Rouse segment—the emergence of the entropic slow mode is indeed very intriguing. The energetic nature of the fast mode and the entropic nature of the slow mode are analyzed below in detail. For the sake of simplicity, we will consider the Fraenkel dumbbell case; then, the extension of the analysis to a Fraenkel chain with more than two beads will be discussed.

If there is no attractive interaction potential between two beads, the thermal fluctuations in an equilibrium state will eventually separate them far apart. Therefore, at equilibrium the average distance between the two beads (or the average distance over a long period of time) is not that corresponding to the tensionless point of the potential—namely, when the bond length is equal to b_0 in the case of the Fraenkel segment—but larger. There are different ways to define the average as will be discussed below; however, this is true in all cases. Hence, the two beads are each more often than not under a tension to bring them closer. This is so with a Rouse segment as well as with a Fraenkel segment. These tensile forces on the bonds play important roles contributing to the stress tensor of the chain. Because the Fraenkel potential rises up sharply with a deviation from the tensionless point, the average bond length in the equilibrium state should be larger than b_0 by only a small amount δ_0. Physically, δ_0 being small is responsible for the existence of the entropy-driven slow mode; with δ_0 being small, in an approximate way, the tensile force on the segment may be expressed as a linear function of the bond vector as occurring in the Rouse theory.

For the Fraenkel dumbbell, the Langevin equation in terms of the bond vector, $\mathbf{b}(t)=\mathbf{R}_2(t)-\mathbf{R}_1(t)$, is given by

$$\frac{d\mathbf{b}(t)}{dt}=-\left(\frac{2}{\zeta}\right)\frac{H_F}{b_0^2}\left[1-\frac{b_0}{|\mathbf{b}(t)|}\right]\mathbf{b}(t)+\mathbf{g}(t), \tag{15}$$

where the fluctuation term is given by $\mathbf{g}(t)=\mathbf{g}_2(t)-\mathbf{g}_1(t)$, with $\mathbf{g}_1(t)$ and $\mathbf{g}_2(t)$ being the fluctuations on beads 1 and 2, respectively.

Equation (15) can be similarly expressed in the discrete form for simulation purpose as described in Sec. II. Defining

$$1-\frac{b_0}{|\mathbf{b}(t)|}=\frac{\delta(t)}{b_0}, \tag{16}$$

Eq. (15) is rewritten as

$$\frac{d\mathbf{b}(t)}{dt}=-\left(\frac{2}{\zeta}\right)\frac{H_F}{b_0^3}\delta(t)\mathbf{b}(t)+\mathbf{g}(t). \tag{17}$$

Corresponding to Eq. (17), the xy shear stress component is given by

$$J_{xy}(t)=-\frac{H_F}{b_0^3}\delta(t)b_x(t)b_y(t). \tag{18}$$

Hence

$$G_S(t)=\frac{1}{kT}\langle J_{xy}(0)J_{xy}(t)\rangle$$

$$=\frac{H_F^2}{kTb_0^6}\langle\delta(0)b_x(0)b_y(0)\delta(t)b_x(t)b_y(t)\rangle. \tag{19}$$

As expected, the simulation results obtained for the Fraenkel dumbbell based on the combination of Eqs. (7) and (8) and on Eq. (19) are identical. In the simulation, the fluctuation in $\delta(t)$ as defined by Eq. (16) can be monitored separately al-

lowing the time-correlation function $\langle \delta(0)\delta(t)\rangle$ to be calculated. Physically, $\delta(t)$ approximately represents the deviation of $|\mathbf{b}(t)|$ from b_0. Any small change in $|\mathbf{b}(t)|$ leads to a large relative change in $\delta(t)$; for instance, a change in $|\mathbf{b}(t)|$ from 1.005 to 1.01 doubles the value of $\delta(t)$. As a result, compared to the motion associated with the bond vector $\mathbf{b}(t)$ itself (mainly reorientational motion), $\delta(t)$ represents fast fluctuations with large relative fluctuation amplitude, giving rise to a fast relaxation process in $G_S(t)$ as shown below. As $\delta(t)$ originates from the particular form of Fraenkel potential, representing the fluctuations in the tension on the Fraenkel segment, the fast relaxation mode may be very well referred to as an energetic-interactions-driven dynamic process. Because of the large difference between the fluctuation rate of $\delta(t)$ and that associated with $b_x(t)b_y(t)$, Eq. (19) may be approximated by

$$G_S(t) \approx \frac{H_F^2}{kTb_0^6}\langle \delta(0)\delta(t)\rangle\langle (b_x(0)b_y(0))(b_x(t)b_y(t))\rangle$$
$$= \frac{H_F^2}{kTb_0^6}[\langle \Delta\delta(0)\Delta\delta(t)\rangle + \delta_0^2]\langle (b_x(0)b_y(0))$$
$$\times (b_x(t)b_y(t))\rangle, \tag{20}$$

where formally

$$\delta(t) = \Delta\delta(t) + \delta_0, \tag{21}$$

with

$$\langle \Delta\delta(t)\rangle = 0, \quad \text{and } \langle \delta(t)\rangle = \delta_0. \tag{22}$$

As explained above, δ_0 is greater than zero. Equation (20) suggests two distinct relaxation processes in $G_S(t)$, as observed. At long times when $\langle \Delta\delta(0)\Delta\delta(t)\rangle$ has diminished, $G_S(t)$ as given by Eq. (20) transits into a slow-relaxing region, which would be described by

$$\frac{1}{kT}\langle J_{xy}(0)J_{xy}(t)\rangle = \frac{H_F^2}{kTb_0^6}[\delta_0^2]\langle (b_x(0)b_y(0))(b_x(t)b_y(t))\rangle. \tag{23}$$

In the short-time region where the process $\langle \Delta\delta(0)\Delta\delta(t)\rangle$ is dominant, the approximation as used in Eq. (20) is expected to be good. By contrast, over a long period of time, as the nonvanishing residual fluctuations in $\delta(t)$ are small and more comparable in (relative) magnitude to the slow fluctuations in $b_x(t)b_y(t)$, the separation into the product of δ_0^2 and $\langle (b_x(0)b_y(0))(b_x(t)b_y(t))\rangle$ as done in Eq. (23) may not be well justified. Nevertheless, the approximate form as given by Eq. (20) helps us understand the coexistence of the fast and slow modes of motion as distinctly observed from the simulation. To illustrate the results of the approximation form and at the same time somewhat make up for the deficiency of the approximation as represented by Eq. (20) in the long-time region, we set the base line of $\langle \delta(0)\delta(t)\rangle$ in two different ways, from which an approximate $G_S(t)$ curve in each case can be obtained for comparison with the exact result—such analyses help reveal the key physical elements that affect $G_S(t)$. One is determined by the natural base line of $\langle \delta(0)\delta(t)\rangle$, which, denoted by $\delta_0^2 = \delta_N^2$, is found to be 4×10^{-6}. The second is the addition of an adjustable parameter δ_x^2 on top of the natural base line δ_0^2 of the correlation function $\langle \delta(0)\delta(t)\rangle$ such that a close fitting to the exact $G_S(t)$ curve [obtained from using Eq. (19)] can be obtained. The best δ_x value is found to be 0.008. The $G_S(t)$ curves calculated without and with $\delta_x^2 = 6.4\times10^{-5}$ added are compared with the exact result in Fig. 4. The corresponding $\langle \delta(0)\delta(t)\rangle$ and $\langle \delta(0)\delta(t)\rangle + \delta_x^2$ curves are shown in Fig. 5. With $\delta_x^2 = 6.4\times10^{-5}$ added, the total base line becomes $\delta_F^2 = \delta_0^2 + \delta_x^2 = 6.8\times10^{-5}$. It is interesting to note that $\delta_F = 0.008\,25$ is only larger by 10% than the value of 0.0075 (denoted by δ_V) expected from considering the virial theorem.[37] As described in the Appendix, the virial theorem is well confirmed in our simulation.

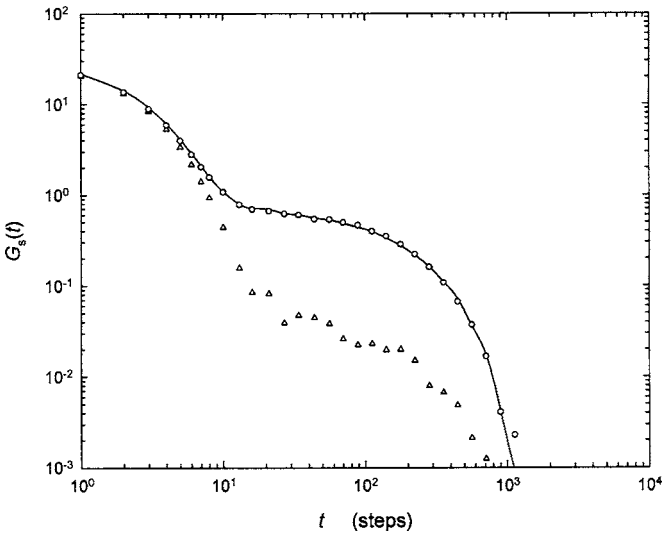

FIG. 4. The equilibrium-simulation $G_S(t)$ curves of the Fraenkel dumbbell: exact [using Eq. (19);—] and approximations [△, using Eq. (20) with $\delta_0^2 = \delta_N^2 = 4\times10^{-6}$ as the base line of $\langle \delta(0)\delta(t)\rangle$ and ○ using Eq. (20) with $\delta_x^2 = 6.4\times10^{-5}$ added to the base line].

One can notice that the fast declines occurring in the early parts of $G_S(t)$ and $\langle \delta(0)\delta(t)\rangle$ (or $\langle \delta(0)\delta(t)\rangle + \delta_x^2$) have the same time scale and that there is virtually no difference

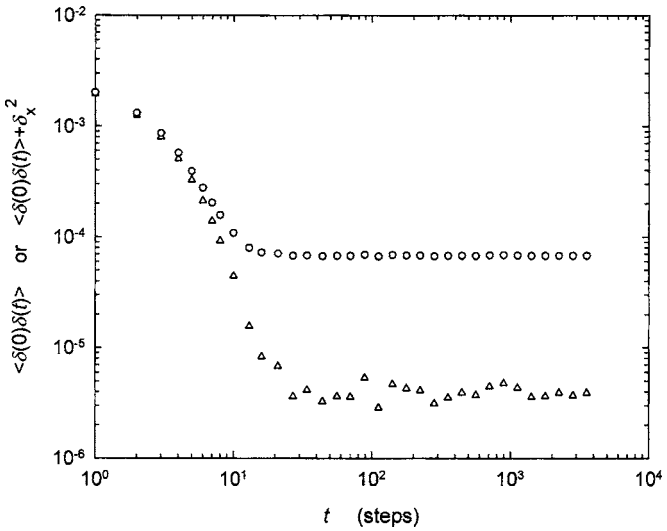

FIG. 5. Time-correlation functions $\langle \delta(0)\delta(t)\rangle$ or $\langle \delta(0)\delta(t)\rangle + \delta_x^2$ obtained from simulation on the Fraenkel dumbbell with $\delta(t)$ defined by Eq. (16): △ with $\delta_0^2 = \delta_N^2 = 4\times10^{-6}$ and ○ with $\delta_x^2 = 6.4\times10^{-5}$ added to the base line.

between the simulation results calculated with and without $\delta_x^2=6.4\times10^{-5}$ added. Clearly this is due to the mean square of the fluctuation magnitude, $\langle\delta(0)\delta(0)\rangle$, being much larger than δ_x^2. For $G_S(t)$, the approximate results are also virtually indistinguishable from the exact one in most part of the fast-mode region—the early portion. Clearly, these agreements occurring in the short-time region are due to the dominant effect of $\langle\Delta\delta(0)\Delta\delta(t)\rangle$ and indicates that the fast mode in $G_S(t)$ arises from the segment-tension fluctuation $\delta(t)$—therefore an energetic-interactions-driven dynamic process. In the long-time region, large divergences between the curves calculated with and without $\delta_x^2=6.4\times10^{-5}$ added occur in both $G_S(t)$ and $\langle\delta(0)\delta(t)\rangle$ (or $\langle\delta(0)\delta(t)\rangle+\delta_x^2$). Because the separation of δ_0^2 from $\langle(b_x(0)b_y(0))(b_x(t)b_y(t))\rangle$ [Eq. (23)] is not a well-justified approximation as explained above, using the natural base line of $\langle\delta(0)\delta(t)\rangle$—namely, $\delta_0^2=\delta_N^2=4\times10^{-6}$, which is much smaller than the value of δ_V^2 or δ_F^2—leads to the poorest result. With $\delta_F^2=6.8\times10^{-5}$ (i.e., with $\delta_x^2=6.4\times10^{-5}$ added), the simulation result of using the approximate form gives a $G_S(t)$ curve which is virtually indistinguishable from that obtained from using the exact form.

We may shift our attention to the long-time approximate $G_S(t)$ functional form [Eq. (23)] itself. Equation (23) represents the time-correlation function of the stress tensor component $J_{xy}(t)$ in the long-time region described by the Langevin equation:

$$\frac{d\mathbf{b}(t)}{dt}=-\left(\frac{2}{\zeta}\right)\frac{H_F\delta_0}{b_0^3}\mathbf{b}(t)+\mathbf{g}(t), \tag{24}$$

which is linear and of the same form as that of the Rouse dumbbell:

$$\frac{d\mathbf{b}(t)}{dt}=-\frac{6kT}{\zeta\langle\mathbf{b}^2\rangle_R}\mathbf{b}(t)+\mathbf{g}(t). \tag{25}$$

Thus, the slow mode is expected to behave very similarly to the single mode of motion in the Rouse dumbbell. If the δ_V value as obtained from the virial theorem [$\delta_V=3kTb_0/H_F$, as from Eq. (A1)] is used for δ_0, Eqs. (24) and (25) become identical with $b_0=\langle\mathbf{b}^2\rangle_R^{1/2}=1$ as set in this study and will lead to the same time-correlation function of the bond vector as given by the Rouse dumbbell model:[3]

$$\langle\mathbf{b}(0)\cdot\mathbf{b}(t)\rangle=\langle\mathbf{b}^2\rangle_R\exp\left(-\frac{t}{\tau}\right), \tag{26}$$

with

$$\tau=\frac{\zeta\langle\mathbf{b}^2\rangle_R}{6kT}=\frac{\zeta b_0^2}{2H_F(\delta_V/b_0)}. \tag{27}$$

[Note: Obtained from the simulation, the mean square bond length $\langle\mathbf{b}^2\rangle$ of the Fraenkel dumbbell is greater than that of the Rouse dumbbell $\langle\mathbf{b}^2\rangle_R$ by only 1.3%—this small difference will occur in the zero-time value of Eq. (26); as this difference is very small, particularly, much smaller than the difference between δ_N, δ_V, and δ_F, it is neglected here.] The shape of the $\langle\mathbf{b}(0)\cdot\mathbf{b}(t)\rangle$ curve from the simulation is well described by the single exponential form just as that of the Rouse dumbbell model but with a relaxation time longer by about 45%. In other words, using the relaxation time of $\langle\mathbf{b}(0)\cdot\mathbf{b}(t)\rangle$ as the criterion for determining δ_0, the best value, denoted by δ_τ, should be 0.0052.

The close fit of the approximation $G_S(t)$ result to the exact as obtained and shown in Fig. 4 gives $\delta_F=0.008\,25$, which is only slightly larger than $\delta_V=0.0075$. As opposed to giving a slight underestimate in this case, the virial theorem gives an overestimate of the δ_0 value when the relaxation time of the time-correlation function $\langle\mathbf{b}(0)\cdot\mathbf{b}(t)\rangle$ is used as the criterion. Involving only a very small approximation [see Eq. (A1)] which is unrelated to the separation into two time-correlation functions as done in Eq. (20), δ_V from the virial theorem can be regarded as independent and trustworthy. As opposed to the independence of δ_V, each of the equations [Eqs. (20), (23), and (24)] as involved in estimating the δ_N, δ_τ, and δ_F values contains an element of approximation, which naturally distorts the real situation in different ways; the obtained δ_N, δ_τ, and δ_F values are not expected to be the same. Excluding the δ_N value, which is apparently based on a bad approximation, the obtained δ_τ and δ_F values are within 30% of their average, which is very close to the value δ_V from the virial theorem. The closeness of these estimated values to the expectation based on the virial theorem supports that the approximations involved in the above analyses are well justified and that the physical picture they present–the fast mode in $G_S(t)$ is an energetic-interactions-driven dynamic process and the slow mode is an entropy-driven one as the Rouse modes of motion–is a valid description. The described basic natures associated with the fast and slow modes, respectively, will be further shown in a different way in the discussion of the step-strain-simulation $G_S(t)$ below.

For a Fraenkel chain with more than two beads, the extension of the above analysis requires an examination. As opposed to Eq. (19) for a dumbbell, for an N-bead chain, the relaxation modulus is given by

$$\begin{aligned}G_S(t)&=\frac{1}{(N-1)kT}\langle J_{xy}(0)J_{xy}(t)\rangle\\&=\frac{H_F^2}{(N-1)kTb_0^6}\left\langle\left(\sum_{i=1}^{N-1}\delta_i(0)b_{ix}(0)b_{iy}(0)\right)\right.\\&\quad\left.\times\left(\sum_{j=1}^{N-1}\delta_j(t)b_{jx}(t)b_{jy}(t)\right)\right\rangle.\end{aligned} \tag{28}$$

As being dynamically correlated, the contributions of the cross terms in Eq. (28) to $G_S(t)$ are not zero. Such dynamic cross correlation is also expected in the Rouse-chain model.[38] As a result, applying the above conclusions for a Fraenkel dumbbell to an N-bead chain requires an analysis. As it turns out, the self-terms of Eq. (28) as given by

$$G_S^{\text{self}}(t)=\frac{H_F^2}{(N-1)kTb_0^6}\sum_{i=1}^{N-1}\langle\delta_i(0)b_{ix}(0)b_{iy}(0)\delta_i(t)b_{ix}(t)b_{iy}(t)\rangle \tag{29}$$

are virtually the solely contributing terms to $G_S(t)$ in the short-time region; in other words, the cross terms only contribute to the long-time region. This is illustrated by the com-

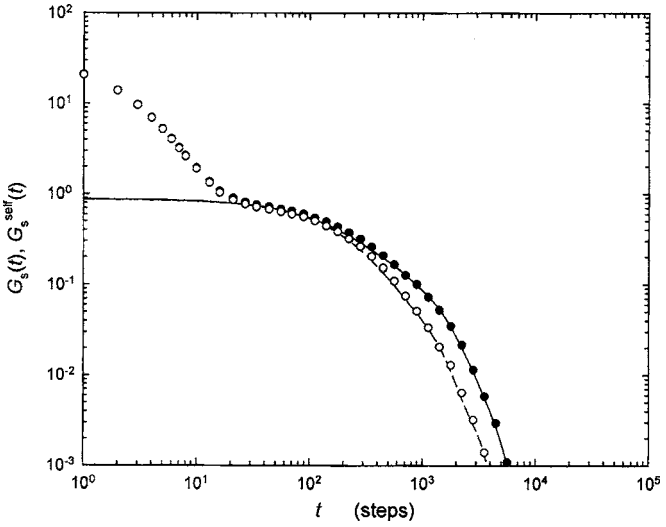

FIG. 6. Comparison of the equilibrium-simulation $G_S(t)$ [● based on Eq. (28)] and $G_S^{self}(t)$ [○ based on Eq. (29)] for the five-bead Fraenkel chain; also shown are the equilibrium-simulation $G_S(t)$ (—) and $G_S^{self}(t)$ (---) for the five-bead Rouse chain.

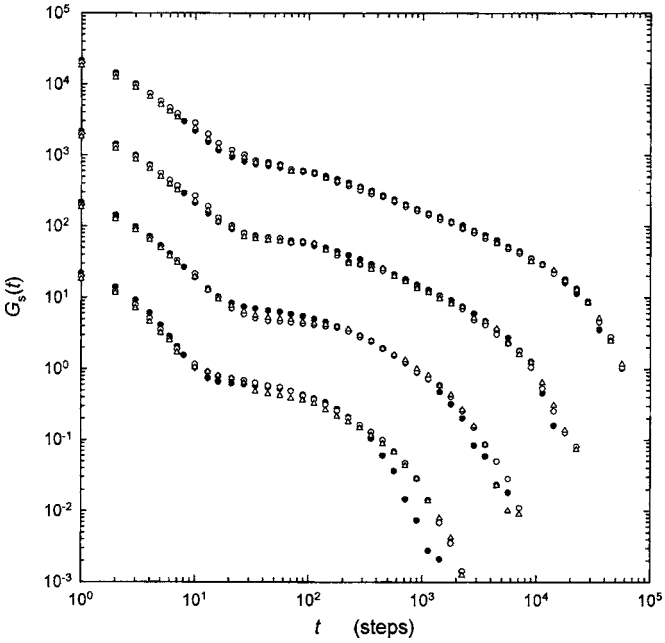

FIG. 7. Comparison of the step-strain-simulation $G_S(t)$ curves for the 2-bead, 5-bead, 10-bead, and 20-bead Fraenkel chain at $\lambda=0.2$ (△) and 0.5 (○) with the equilibrium-simulation curve (●). To avoid overlapping of points for different curves, the results of $N=5$, 10, and 20 have been shifted upwards by one, two, and three decades, respectively.

parison of the curves of $G_S(t)$ and $G_S^{self}(t)$ for a five bead chain in Fig. 6. As also shown in the same figure, virtually the same relative weight between the self- and cross terms in the long-time region occurs to the Rouse-chain model, further supporting the Rouse-chain behavior of the slow mode. Since there is virtually no difference between $G_S(t)$ and $G_S^{self}(t)$ in the short-time region for the Fraenkel chain, we may use Eq. (29) to illustrate the effect of fluctuations in $\delta_i(t)$, which is dominant in the short-time region. Since the summation in Eq. (29) just represents a multiple of the single term in Eq. (19), the analysis based on the Fraenkel dumbbell as presented above can be readily applied to an N-bead chain. Thus, the conclusions of the analysis based on the Fraenkel dumbbell as to the energetic-interactions-associated nature of the fast mode in $G_S(t)$ are basically equally applicable to the Fraenkel chains in general with multiple beads.

In the slow-mode region, the contributions of the cross terms clearly cannot be neglected. This together with the lack of a good justification for separating $\langle\delta(0)\delta(t)\rangle$ from $\langle(b_x(0)b_y(0))(b_x(t)b_y(t))\rangle$ in the long-time region makes an analysis for the slow mode similar to that done to the Fraenkel dumbbell unwieldy. Nevertheless, the entropic nature of the slow mode is clearly supported by the fact that the slow mode is well described by the Rouse theory in all aspects as shown above. Furthermore, through the fluctuation-dissipation theorem, it is found from the simulation of $G_S(t)$ following a step strain as discussed below that the slow mode should arise from fluctuations in the segmental-orientation anisotropy—an entropic origin.

IV. STEP-STRAIN-SIMULATION $G_S(t)$

Based on the fluctuation-dissipation theorem, the step-strain-simulation $G_S(t)$ in the linear region of the applied strain is expected to be equivalent to the equilibrium-simulation $G_S(t)$. In Fig. 1, the step-strain-simulation $G_S(t)$ curves obtained at $\lambda=0.5$ for two-bead, five-bead, and ten-bead Rouse chains are also shown. As expected from the theory, no nonlinear effect can be observed between the $G_S(t)$ curves obtained from the simulations at $\lambda=0.5$ and 1 for the Rouse-chain model; in other words, the shown step-strain-simulation $G_S(t)$ curves are linear results. These step-strain-simulation results are in close agreement with the equilibrium-simulation and Rouse theoretical curves, illustrating the working of the fluctuation-dissipation theorem and confirming the validity of the simulations as presented in this study.

The equilibrium-simulation $G_S(t)$ and the step-strain-simulation $G_S(t)$ curves obtained at $\lambda=0.2$ and 0.5 for the 2-bead, 5-bead, 10-bead, and 20-bead Fraenkel chains are compared in Fig. 7. There are clear differences between the equilibrium-simulation $G_S(t)$ and the step-strain-simulation $G_S(t)$ at $\lambda=0.2$ in the cases of two-bead and five-bead chains, indicating that the fluctuation-dissipation theorem is not fulfilled totally as in the Rouse-chain case. This may be due to $\lambda=0.2$ being not in the linear region yet as there is some small difference between the $G_S(t)$ results at $\lambda=0.2$ and 0.5 in the fast-mode region. In fact, the numerically calculated $G_S(0)$ as a function of the strain λ as shown in Fig. 6 of the companion paper[30] indicates that rigorously the linear region should occur below $\lambda=0.005$. However, further investigation by decreasing the λ value indicates that this is not the main cause. With the λ value decreasing, the number of repeating cycles required to obtain a well-averaged $G_S(t)$ curve increases greatly. Prevented by the overwhelmingly long computer time involved, we limit our study to the Fraenkel dumbbell system—where the difference from the equilibrium-simulation $G_S(t)$ is also the most obvious—in comparing the $G_S(t)$ results at $\lambda=0.004$ and 0.2. Although there are very small differences between the results at $\lambda=0.004$ and 0.2, the $G_S(t)$ result of the Fraenkel dumbbell at

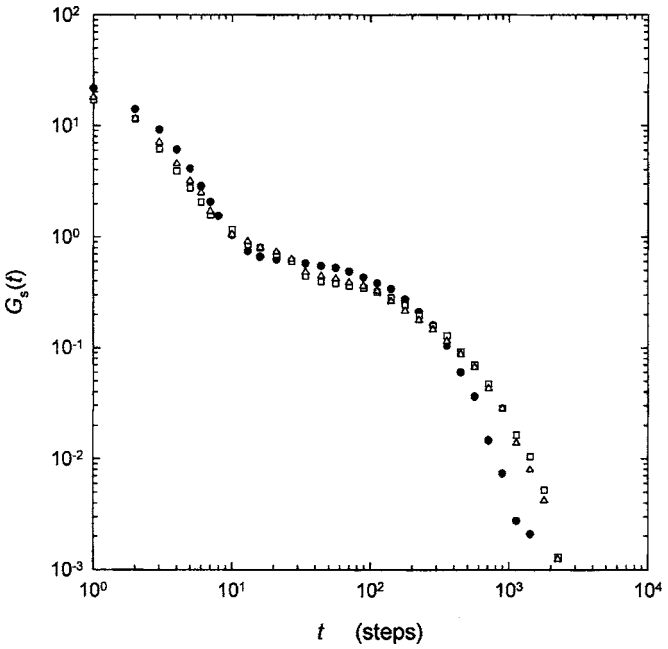

FIG. 8. Comparison of the step-strain-simulation $G_S(t)$ curves for the Fraenkel dumbbell at $\lambda=0.004$ (□) and 0.2 (△) with the equilibrium-simulation curve (●).

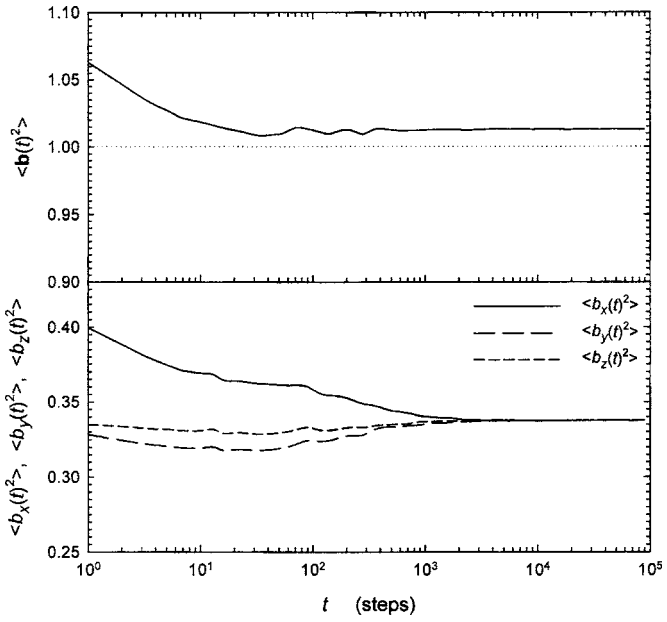

FIG. 9. The time-step dependences of $\langle \mathbf{b}^2(t)\rangle$ and the components $\langle b_x^2(t)\rangle$, $\langle b_y^2(t)\rangle$, and $\langle b_y^2(t)\rangle$ for the five-bead Fraenkel chain following a step strain $\lambda=0.5$.

$\lambda=0.004$ does not appear to be closer to the equilibrium-simulation result as shown in Fig. 8. Summarizing the results shown in Figs. 7 and 8, differences between the equilibrium-simulation and step-strain-simulation $G_S(t)$ curves occurs mainly in the cases of $N=2$ and 5, and virtually no differences can be observed when $N=10$ and 20 even though $\lambda=0.2$ and 0.5 are not really in the linear region. In the case of $N=2$, while the whole shapes of $G_S(t)$ curves are very similar, differences can be observed in different regions. In the case of $N=5$, the difference begins to appear in an obvious way in the early part of the slow mode, where an effect related to the coupling between $\delta(t)$ and $b_x(t)b_y(t)$—a subject discussed in Sec. III—is most likely to occur. The results of $N=5$ suggest that the coupling between $\delta(t)$ and $b_x(t)b_y(t)$ may occur differently in the two types of simulations. This is also suggested by the similarity of the trends that can be observed in Figs. 3 and 7, as explained in the following. The results shown in Fig. 7 indicate that the agreement between the equilibrium-simulation and step-strain-simulation $G_S(t)$ curves improves greatly as N increases. Similarly, as shown in Fig. 3, the shift factor along the modulus coordinate involved in superposing the Rouse theoretical curve on the equilibrium-simulation $G_S(t)$ curve approaches the perfect value 1 as N increases. As being more removed from the fast mode, the lower modes (of the slow mode) in an N-bead chain may improve the overall decoupling of the fast and slow modes as N increases. In other words, the trend in Fig. 3 suggests that the coupling between $\delta(t)$ and $b_x(t)b_y(t)$ is effectively reduced, making the slow mode better described by the Rouse theory as the number of modes of motion in the slow mode increases. As the difference in coupling may be reduced by the decrease in the coupling itself, this leads to the better agreement between the equilibrium-simulation and step-strain-simulation $G_S(t)$ curves as N increases. When $N=2$ or 5, in spite of the visible differences, we still see an overall agreement between the equilibrium-simulation and step-strain-simulation $G_S(t)$ curves, each revealing clearly two separate modes. We refer to such an overall agreement as a quasiversion of the fluctuation-dissipation theorem.

In Fig. 9, we show the mean square segment length $\langle \mathbf{b}^2(t)\rangle$ and its components, $\langle b_x^2(t)\rangle$, $\langle b_y^2(t)\rangle$, and $\langle b_y^2(t)\rangle$, of a five-bead Fraenkel chain as a function of time following the application of the step shear strain $\lambda=0.5$. Although $\lambda=0.5$ is farther away from the linear region than $\lambda=0.2$, we show these results because their changes with time are more discernible and at the same time, the corresponding $G_S(t)$ curve does not differ from the one obtained from the equilibrium simulation very much. Comparing these results can better serve our purpose, as discussed below, than showing the results at $\lambda=0.2$. As shown in Fig. 9, the segment length is stretched by the step strain and relaxes back to the equilibrium value, as opposed to the segment length fluctuating around its mean value in the equilibrium simulation. From comparing the time scales of the dramatic declines in the early part of $G_S(t)$ (Fig. 7) and $\langle \mathbf{b}^2(t)\rangle$ (Fig. 9), it is clear that the fast mode occurring in the step-strain-simulation $G_S(t)$ clearly reflects the decrease of the average segment length back to the equilibrium value and the corresponding reduction of the tension on the segments. This segment-tension relaxation corresponds to the time-correlation function of segment-tension fluctuation, $\langle \delta(0)\delta(t)\rangle$, as shown in Fig. 5. It is interesting to note that right after $\langle \mathbf{b}^2(t)\rangle$ has completed its first fast decline, it displays signs of overshooting and oscillation around the equilibrium value before reaching the final stable (equilibrium) value. The oscillation should be part of the coupling between $\delta(t)$ and $b_x(t)b_y(t)$ which is most noticeable in the early part of the slow mode as suggested in Sec. III.

Following a step strain $\lambda=0.5$, in the early part of the

slow mode in $G_S(t)$, the mean square segment length $\langle \mathbf{b}^2(t) \rangle$ has declined to a level (including the oscillation zone as can be noticed in Fig. 9) which has the same average value as that occurring all the time in the equilibrium simulation. In the same time region, however, as the differences between the time dependences of the components $\langle b_x^2(t) \rangle$, $\langle b_y^2(t) \rangle$, and $\langle b_y^2(t) \rangle$ indicate, there is some net orientation anisotropy as opposed to maintaining isotropy in average in the equilibrium-simulation case. As orientation does not cause a change in the potential energy on the segment, the anisotropy of the segmental orientation leads to the entropic nature of the slow mode. According to the fluctuation-dissipation theorem, corresponding to the randomization of segmental-orientation anisotropy occurring in the slow-mode region as revealed from the simulation following a step shear deformation, fluctuations in segmental orientation should be present all the time in the equilibrium state, which should be responsible for the entropic slow mode in the equilibrium-simulation $G_S(t)$. The close correlation between the slow mode in $G_S(t)$ and the segmental-orientation anisotropy as further revealed in the nonlinear region of strain will be analyzed in greater detail in the companion paper.[30]

V. COMPARISON OF SIMULATION WITH EXPERIMENT

Both the Rouse theory and the Monte Carlo simulation using the Rouse-chain model or the Fraenkel-chain model are a mean-field representation, meaning that the relaxation modulus of an entanglement-free polymer system (concentrated solution or melt) is the sum of contributions from all the chains in a unit volume, each being represented by its statistically averaged time dependence. In comparison with experimental results of polymer melts,[3–5,25] the mean-field representation works very well in the long-time or entropic region of the relaxation modulus, as illustrated by the quantitative agreement of the measured viscoelastic spectra with the Rouse theory. Since there is basically no difference in the entropic region between the Rouse theory and the simulation result of the Fraenkel chain with $N \gg 2$, and the overall $G_S(t)$ line shape of the Fraenkel chain is very similar to that typically observed experimentally, we may compare the simulation result with experiment over the whole time range. Such a comparison would shed light on how well the key features of the relaxation modulus in the short-time region—the structural-relaxation process—can be captured by the Fraenkel-chain model. Intuitively, the mean-field Fraenkel-chain model should be an oversimplified representation for the viscoelastic behavior in the structural-relaxation region for a polymer in its melt state.

Recently the relaxation modulus curves of an entanglement-free nearly monodisperse polystyrene melt have been obtained from its creep compliance $J(t)$ measured by Plazek and O'Rourke[19] at different temperatures. $J(t)$ can be converted to the relaxation modulus $G(t)$ through the basic equation of linear viscoelasticity:

$$t = \int_0^t J(t')G(t-t')dt'. \tag{30}$$

The convolution integral of Eq. (30) can be solved numerically by the method of Hopkins and Hamming,[39,40] as detailed in Appendix A of Ref. 15. The experimental $J(t)$ curves have been quantitatively fitted by curves calculated through Eq. (30) using a $G(t)$ functional form which incorporates a stretched exponential form for the glassy-relaxation (structural-relaxation) process into the Rouse theory,[25] as expressed by

$$G(t) = A_G^f \mu_G(t) + \rho RT \int \frac{f(M)}{M} \mu_R(t,M) dM, \tag{31}$$

where $\mu_R(t,M)$ is given by Eq. (10); ρ, R, and T are the density, gas constant, and absolute temperature, respectively; $f(M)$ represents the molecular-weight distribution of the sample, and A_G^f is the full relaxation strength of the glassy-relaxation process $\mu_G(t)$, phenomenologically expressed by

$$\mu_G(t/\tau_G) = \exp(-(t/\tau_G)^\beta), \quad 0 < \beta \leqslant 1. \tag{32}$$

Note that Eq. (31) represents a scheme of analysis using the Rouse theory as the reference frame for characterizing the glassy-relaxation process occurring in the short-time region. The scheme is equivalent to that using the successful description of the rubber(like)-to-fluid region by the ERT as the reference frame for entangled systems [see Eqs. (1) and (4) of Ref. 15]. Also the separation of the glassy-relaxation process from the Rouse process (or the ERT processes) as assumed in Eq. (31) is equivalent to the basic scheme used by Inoue *et al.*[6–9] in analyzing the dynamic mechanical and birefringence results together in terms of a modified stress-optical rule.

In the quantitative $J(t)$ line-shape analyses, the effect of the molecular-weight distribution $f(M)$ of the studied samples, even though very narrow, need to be included in the calculation. The molecular-weight distribution is assumed to be described by the Schulz function,[41] whose distribution width is characterized by the single parameter $Z(M_w/M_n = (Z+1)/Z)$. As a fitting parameter, the Z values obtained from the quantitative line-shape analyses have always been within the expected range, giving $M_w/M_n \leqslant 1.05$;[3–5,25] for the studied sample $M_w/M_n = 1.05$ (corresponding to $Z=20$) is obtained.[25] As the Monte Carlo simulation carried out in the present study is for an ideally monodisperse system, for making a comparison between experiment and simulation, we use the parameters obtained for the studied nearly monodisperse sample to calculate the $G(t)$ curve expected for the corresponding ideally monodisperse system. The use of the Langevin equation in the present study implies that the system is ergodic.[3,31] Thus, the $G(t)$ line shape at temperatures sufficiently high above T_g is the one that should be used for comparison with the simulation result.

The molecular weight for a single Rouse segment, m, is about 850 for polystyrene;[6–16] the studied sample with $M_w = 16\,400$ is equivalent to a chain with 20 beads in average (see the note in Ref. 42).[42] Shown in Fig. 10 is the comparison of the equilibrium-simulation $G(t)$ curve for 20-bead

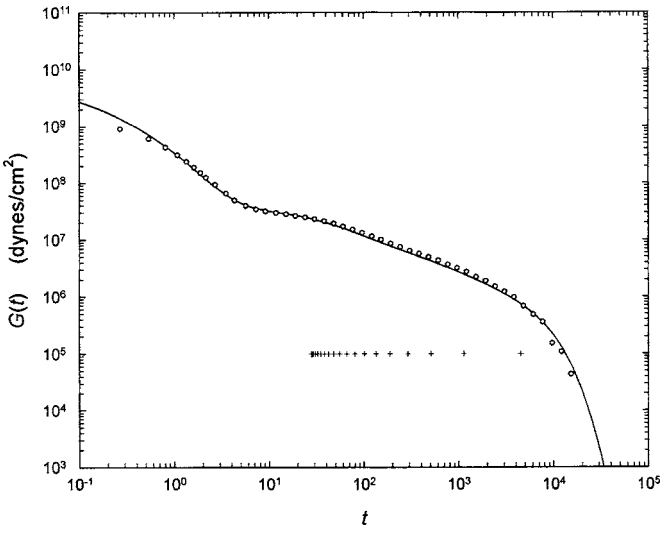

FIG. 10. Comparison of the equilibrium-simulation $G(t)$ curve (○) for the 20-bead Fraenkel chain with $H_F=400kT$ and the expected "experimental" curve (—) for an "ideally monodisperse polystyrene sample" with the molecular weight equivalent to $N=20$; also shown are the points (+) representing the relaxation times of the 19 Rouse normal modes. See the text.

Fraenkel chains with $H_F=400kT$ and the expected "experimental" curve for the ideally monodisperse polystyrene "sample" with molecular weight equal to 16 400 at high temperatures. [Note: although the $G(t)$ line shape is for $T>T_g+40$ °C, the modulus is that corresponding to $T=373$ K.] As shown, the experimental curve is calculated using an arbitrary K value: 10^{-4} [see Eq. (11)], and the simulation curve has been multiplied by a proper factor in both the modulus and time coordinates to obtain a close superposition between the two curves. As the shift factor along the time coordinate depends on the K value used in the calculation and the step length d employed in the simulation [see Eq. (12)], its value is not of particular interest. However, the shift factor along the modulus coordinate is much related to the entropic nature of the slow mode as discussed in Sec. III regarding the results shown in Fig. 3. The vertical multiplication factors used for obtaining the close superposition is 4.2×10^7, which is very near the value of 3.8×10^7 expected if the entropic region of the simulation $G(t)$ is in perfect agreement with the Rouse theory. The ratio of 3.8/4.2 also agrees closely with the value of 0.95 used to superpose the Rouse theoretical curve on the simulation $G_S(t)$ curve of the 20-bead Fraenkel chain shown in Fig. 3. Some of the small difference may be due to the fact that only one adjustable parameter—the shift along the modulus coordinate is involved in the superposition made in Fig. 3 while shifts in both the time and modulus coordinates are allowed in Fig. 10. The agreement in the general shape between the two $G(t)$ curves is indeed very encouraging, considering the simplicity of the chain model used in the simulation. The choice of the H_F value mainly has an effect on the modulus level as well as the relaxation in the fast-mode region; an increase in H_F leads to higher modulus values in the very short-time region and causes a faster decline in the later part of the fast mode. As the mean-field Fraenkel-chain model should be too simple to describe adequately the viscoelastic behavior of a polymer melt in the energetic-interactions region, a fine tuning of the H_F value may not serve a particularly meaningful purpose. More importantly, the simulation result indicates that the Fraenkel chain with a finite H_F value can describe the generic coexistence of the fast energetic-interactions-driven and slow entropy-driven modes in the experimental $G(t)$. This suggests that a Kuhn segment that can be calculated from the unperturbed mean square end-to-end and fully extended end-to-end distances—static properties—of a polymer should not be totally rigid as far as the dynamic properties, such as viscoelasticity, of the polymer is concerned. Physically, force constants on the various chemical bonds and bond angles (responsible for the vibration modes) and the potential barriers impeding the internal rotations in the microstructure of the polymer may provide such elasticity on a chain domain of size as that of a Kuhn segment.

VI. DISCUSSION

In contrast to the glassy-relaxation process being incorporated phenomenologically into the Rouse theory as expressed in Eq. (31), the segment-tension relaxation process emerges naturally on top of the slow mode in the simulated $G_S(t)$ curves for the entanglement-free Fraenkel chains as presented in this study. Very significantly, as the curves calculated from the Rouse theory which individually describe very well the slow modes of chains with different numbers of beads, N, are each based on a chain with the corresponding N, the close agreement between simulation and theory indicates that the size of the Fraenkel segment is the same as that of the Rouse segment. In other words, this result strongly suggests that the chain domain that can be properly assigned as a "Rouse segment" for describing the linear viscoelastic behavior in the entropic region actually has a considerable degree of rigidity. Such a conclusion is also supported by the study in the nonlinear region of strain as reported in the companion paper.[30] As shown in the present and companion papers, the fluctuation in or randomization of the segmental-orientation anisotropy is responsible for the entropic nature of the slow mode; thus, in the modeling one does not need to put the entropic-force constant into the segments in order to obtain the modes of motion as occurring in the Rouse theory. The close correlation of the segmental orientation with the entropic nature of the segment is ultimately related to the virial theorem as detailed in the Appendix. This conclusion provides an explanation resolving a long-standing fundamental paradox in the success of modern molecular theories of polymer viscoelasticity developed based on the Rouse segment as the most basic structural unit. The paradox becomes apparent when the entropic-force constant on the Rouse segment is shown to be too soft from considering the persistence length or the Kuhn segment length of a polymer chain. As listed in Table I of Ref. 8, the Rouse segment size m for various polymers is of the same order of magnitude as that of the Kuhn segment M_K. In Ref. 8, based on the observation $m\approx M_K$, Inoue and Osaki have suggested that the Rouse segment likely includes contributions from complicated motions, not included in the Rouse chain as originally developed.[1–3] As one may regard each Fraenkel segment as

basically equivalent to a Kuhn segment, the analyses of the results obtained from the present Monte Carlo simulation have given a detailed picture answering the question raised by Inoue and Osaki.

VII. SUMMARY

In this study, based on the entanglement-free Rouse-chain and Fraenkel-chain models we have carried out Monte Carlo simulations of relaxation modulus for chains with different numbers of beads, N, in the equilibrium state and following a step shear deformation. In the case of the Rouse chain, the validity of the simulation is confirmed by the agreement with the analytical results; the fluctuation-dissipation theorem is also perfectly illustrated by the comparison of results from both kinds of simulations. In the case of the Fraenkel chain, a quasiversion of the fluctuation-dissipation theorem is illustrated when $N=2$ and 5; virtually perfect agreements between the two kinds of simulations have been obtained when $N=10$ and 20 (although the strains $\lambda=0.2$ and 0.5 are not really in the linear region). In all cases, two distinct modes of dynamics in the simulated relaxation modulus curves are revealed, which describe the basic features as typically observed in an experimentally obtained relaxation modulus $G(t)$. The physical natures of the two modes are analyzed in detail: The fast one corresponding to the segment-tension fluctuation or relaxation is classified as an energetic-interactions-driven process, and the slow one well described by the Rouse theory is regarded as entropy driven. As indicated by the close agreements observed in the comparisons of the Rouse theory with the slow mode obtained from the simulation for different chain lengths, N, basically one Fraenkel segment substitutes for one Rouse segment. A very important conclusion derived from this study is that the segmental-orientation anisotropy is responsible for the entropic nature of the slow mode; in other words, the entropic-force constant is not a required element in the Rouse segment. This conclusion resolves a long-standing fundamental paradox in the success of the Rouse-segment-based molecular theories of polymer viscoelasticity, which is best indicated by the result obtained by Inoue and Osaki[8] that the sizes of the Rouse and Kuhn segments are of the same order of magnitude. Furthermore, the general agreement as observed in the comparison of the simulation and experimental results strongly suggests that, even though still being a simple mean-field single-chain model—without contributions from intermolecular interactions—the Fraenkel chain has captured the key element of energetic interactions in a polymer system and may serve as a more realistic substitute for the Rouse model.

ACKNOWLEDGMENTS

This work is supported by the National Science Council (NSC 93-2113-M-009-015 and NSC 94-2113-M-009-002) and the simulations were carried out at the National Center for High-Performance Computing.

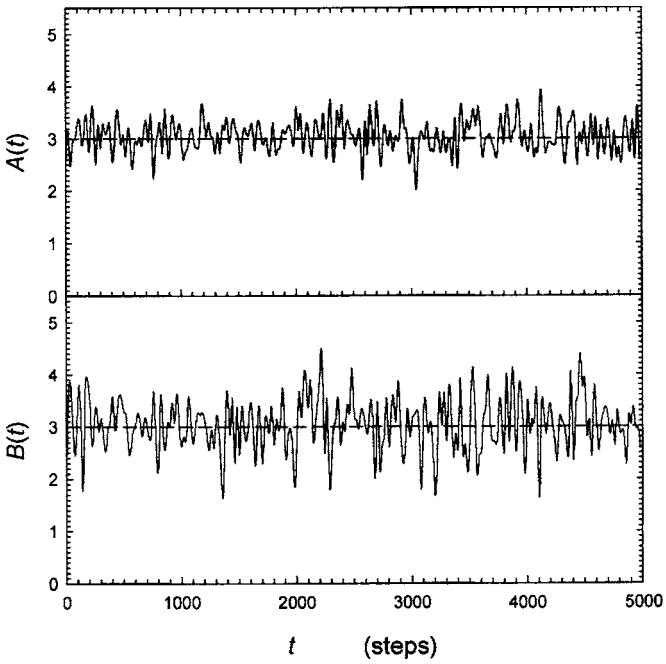

FIG. 11. Fluctuations of the internal kinetic energy for a Fraenkel dumbbell calculated in two different ways as represented by $A(t)=-\Sigma_{i=1}^{2}\mathbf{F}_i(t)\cdot\mathbf{R}_i(t)$ and $B(t)=(H_F/b_0^3)\delta(t)\mathbf{b}(t)\cdot\mathbf{b}(t)$ each in a different equilibrium state, giving average values of 3.073 for A and 3.075 for B; the dash lines are drawn at the value of 3 expected from the virial theorem (with $kT=1$).

APPENDIX: APPLICATION OF THE VIRIAL THEOREM TO THE FRAENKEL DUMBBELL

The average kinetic energy for each degree of freedom being $kT/2$ is a built-in element of the Langevin equation.[32] For simplicity, we consider the Fraenkel dumbbell case; however, the analysis as presented here can be extended to a Fraenkel chain with any number of beads. For a dumbbell, according to the virial theorem[37] $\bar{T}=-(1/2)\Sigma_{i=1}^{2}\overline{\mathbf{F}_i\cdot\mathbf{R}_i}=(H_F/2b_0^3)\overline{\delta(t)\mathbf{b}(t)\cdot\mathbf{b}(t)}$, where $\bar{T}=3kT/2$ is the average internal kinetic energy. This relation is well confirmed by our simulation as shown in Fig. 11. Since as indicted by the simulation $\mathbf{b}(t)\cdot\mathbf{b}(t)$ does not fluctuate more than 10% from its mean value, which is larger than b_0^2 only by less than 1.3%, the virial theorem for the Fraenkel dumbbell can be well represented by

$$\frac{H_F}{b_0}\overline{\delta(t)}=3kT. \tag{A1}$$

For $H_F=400kT$, $\overline{\delta(t)}=0.0075$. In the main text, this $\overline{\delta(t)}$ value is denoted by δ_V.

[1] P. E. Rouse, Jr., J. Chem. Phys. **21**, 1272 (1953).
[2] R. B. Bird, C. F. Curtiss, R. C. Armstrong, and O. Hassager, *Dynamics of Polymeric Liquids*, 2nd ed. (Wiley, New York, 1987), Vol. 2.
[3] Y.-H. Lin, *Polymer Viscoelasticity: Basics, Molecular Theories, and Experiments* (World Scientific, Singapore, 2003).
[4] Y.-H. Lin, Macromolecules **19**, 168 (1986).
[5] Y.-H. Lin and J.-H. Juang, Macromolecules **32**, 181 (1999).
[6] T. Inoue, H. Okamoto, and K. Osaki, Macromolecules **24**, 5670 (1991).
[7] T. Inoue, H. Hayashihara, H. Okamoto, and K. Osaki, J. Polym. Sci., Part B: Polym. Phys. **30**, 409 (1992).
[8] T. Inoue and K. Osaki, Macromolecules **29**, 1595 (1996).
[9] T. Inoue, T. Uematsu, and K. Osaki, Macromolecules **35**, 820 (2002).
[10] Y.-H. Lin, J. Polym. Res. **1**, 51 (1994).

[11] Y.-H. Lin and C. S. Lai, Macromolecules **29**, 5200 (1996).
[12] C. S. Lai, J.-H. Juang, and Y.-H. Lin, J. Chem. Phys. **110**, 9310 (1999).
[13] Y.-H. Lin, J. Chin. Chem. Soc. (Taipei) **49**, 629 (2002).
[14] Y.-H. Lin and Z.-H. Luo, J. Chem. Phys. **112**, 7219 (2000).
[15] Y.-H. Lin, J. Phys. Chem. B **109**, 17654 (2005).
[16] Y.-H. Lin, J. Phys. Chem. B **109**, 17670 (2005).
[17] D. J. Plazek, J. Phys. Chem. **69**, 3480 (1965).
[18] D. J. Plazek, J. Polym. Sci., Part A-2 **6**, 621 (1968).
[19] D. J. Plazek and V. M. O'Rourke, J. Polym. Sci., Part A-2 **9**, 209 (1971).
[20] D. J. Plazek, J. Rheol. **40**, 987 (1996).
[21] D. J. Plazek, Polym. J. (Tokyo, Jpn.) **12**, 43 (1980).
[22] H. Okamoto, T. Inoue, and K. Osaki, J. Polym. Sci., Part B: Polym. Phys. **33**, 417 (1995).
[23] T. Inoue, E. J. Hwang, and K. Osaki, J. Rheol. **36**, 1737 (1992).
[24] K. Adachi and H. Hirano, Macromolecules **31**, 3958 (1998).
[25] Y.-H. Lin (unpublished).
[26] Y.-H. Lin, Macromolecules **17**, 2846 (1984).
[27] Y.-H. Lin, Macromolecules **19**, 159 (1986).
[28] Y.-H. Lin, Macromolecules **20**, 885 (1987).
[29] G. K. Fraenkel, J. Chem. Phys. **20**, 642 (1952).
[30] Y.-H. Lin and A. K. Das, J. Chem. Phys. **126**, 074903 (2007), following paper.
[31] M. Doi and S. F. Edwards, *The Theory of Polymer Dynamics* (Oxford University Press, Oxford, 1986).
[32] D. A. McQuarie, *Statistical Mechanics* (Harper & Row, New York, 1976).
[33] From applying the fluctuation-dissipation theorem, Eq. (7) is the expression for the relaxation modulus based on the molecular expression for the stress tensor as given in Ref. 31 [namely, Eq. (5) here; the sign system used here for the stress tensor is opposite to that used in Ref. 31], which is also in agreement with the expression for the zero-shear viscosity as given in Ref. 32 (page 519). Note: In the Monte Carlo simulation based on the Langevin equation, the velocity distribution is assumed to be at equilibrium, namely, described by the Maxwellian distribution (Refs. 2 and 3); thus, the momentum flux terms only contribute to the isotropic part of the normal stresses and need not be included in the stress expressions in this paper.
[34] H. Vogel, Phys. Z. **22**, 645 (1921); G. S. Fulcher, J. Am. Chem. Soc. **8**, 339; **8** 789 (1925); G. Tammann and G. Hesse, Z. Anorg. Allg. Chem. **156**, 245 (1926).
[35] M. L. Williams, R. F. Landel, and J. D. Ferry, J. Am. Chem. Soc. **77**, 3701 (1955).
[36] J. D. Ferry, *Viscoelastic Properties of Polymers*, 3rd ed. (Wiley, New York, 1980).
[37] H. Goldstein, *Classical Mechanics*, 2nd ed. (Addison-Wesley, Reading, MA, 1980).
[38] Note: For the mean square end-to-end vector of a Fraenkel chain, which is a static property, there is no correlation between different segments, just as in the case of the freely jointed chain. But just as in a Rouse chain, the dynamic coupling between different segments cannot be neglected.
[39] I. L. Hopkins and R. W. Hamming, J. Appl. Phys. **28**, 906 (1957); **29**, 742 (1958).
[40] N. W. Tschoegl, *The Phenomenological Theory of Linear Viscoelastic Behavior* (Springer-Verlag, Berlin, 1989).
[41] G. V. Schulz, Z. Phys. Chem. Abt. B **43**, 25 (1943); L. H. Tung, *Polymer Fractionation*, edited by M. J. R. Cantow (Academic, New York, 1967).
[42] Note: The weight-average molecular weight of the studied polystyrene sample (sample A61[3] in Ref. 19), $M_W=16\,400$, is a little higher than the entanglement molecular weight, $M_e=13\,500$. However, as the molecular-weight distribution of the sample is not extremely narrow, there is a sufficient total amount of entanglement-free components in the distribution to render the whole system entanglement-free; the total weight fraction of components with molecular weights below M_e is calculated from $Z=20$ to be 21%, which causes the entanglement molecular weight for the system to become $M_e'=13\,500/0.79=17\,089$, which is greater than its weight-average molecular weight. As a result, the viscoelastic behavior of the sample in the entropic region has to be analyzed in terms of the Rouse theory rather than the ERT. In the molecular-weight region just above M_e, whether the Rouse theory or the ERT should be used for the line-shape analysis and what Z value should be used for the molecular-weight distribution can only be decided by trial and error. However, the obtained Z value has to be consistent with the choice of the theory. As opposed to using the Rouse theory for this sample, the viscoelastic spectrum of another sample with $M_W=16\,700$ has been quantitatively described by the ERT with $Z=120$ as reported in Refs. 4 and 27.